JLAB-ACC-99-22

DEVELOPMENT OF A CRYOMODULE FOR THE CEBAF UPGRADE*

Jean Delayen# for the Upgrade Cryomodule Development Team,
Jefferson Lab, Newport News, VA 23606, USA

Abstract

Long-term plans for CEBAF at Jefferson Lab call for achieving 12 GeV in the middle of the next decade and 24 GeV after 2010. In support of those plans, an Upgrade Cryomodule, capable of providing more than three times the voltage of the original CEBAF cryomodule specification within the same length, is under development. In particular, this requires the development of superconducting cavities capable of consistently operating at gradients above 12MV/m and Q ~ 10^{10}, new frequency tuners with excellent resolution, and cavity control systems.

1 BACKGROUND

CEBAF was designed and constructed to accelerate an electron beam to 4 GeV by recirculating five times through a pair of 1497 MHz superconducting radio-frequency (SRF) linacs, each providing 400 MeV per pass at an accelerating gradient of 5 MV/m. Isochronous, achromatic 180-degree recirculation arcs connect the two anti-parallel linacs. The design maximum current is 200 μA CW, corresponding to a beam loading current of 1 mA.[1]

From the beginning, the performance of the acceleration system exceeded the design goal.[2] Early in 1996 a one-pass energy of 1 GeV was achieved, and in the spring of 1997 a 90 μA beam was accelerated to 1.16 GeV in a single pass (equivalent to a 5.6 GeV, 18 μA five-pass beam), albeit with stability less than suitable for regular operation. The average accelerating field in the active cavities was 7.8 MV/m, more than 50% above their design field. In the fall of 1997, the full capacity of CEBAF was demonstrated with the delivery of a 4 GeV, 200 μA beam.[3] The initial performance of the CEBAF cavities corresponded to a reliable five-pass energy of about 5 GeV. The performance was predominantly limited by electron field emission that can manifest itself in additional cryogenic losses, x-ray production, and periodic arcs at the cold ceramic window, which is located close to the beam line.[4]

To reduce field emission and increase the operational energy of CEBAF, a program to perform *in situ* helium processing of the cavities was initiated in the fall of 1996 and took place during the scheduled machine shutdown periods in 1997, 1998, and 1999.[3] The *in situ* processing program has increased the installed voltage by about 200 MV, which corresponds to an added voltage of 1 GeV for a five-pass beam, and it is expected that the additional gain will allow operation just above 6 GeV. Starting in the spring of 1999, the accelerator was routinely delivering 5.56 GeV beams for physics experiments.

2 CAVITY AND CRYOMODULE REQUIREMENTS

2.1 Tunnel Layout

The CEBAF energy upgrade to 12 and then 24 GeV will be accomplished within the existing accelerator tunnel. The 12 GeV upgrade will be accomplished using an additional pass through one of the two linacs for a total of five and one-half passes, or eleven linac transits. Each of the linacs has five module positions that were left empty during CEBAF construction (Figure 1). These ten positions will be filled with Upgrade Cryomodules. Six existing cryomodules in the linacs and the two injector cryomodules will be replaced.

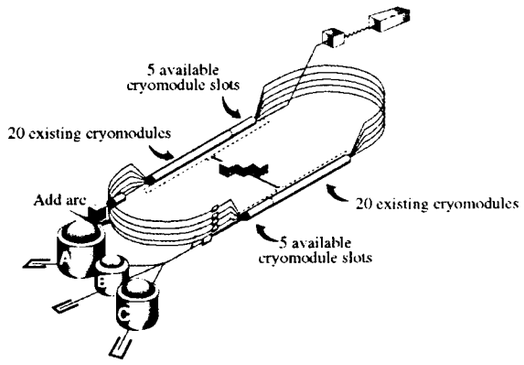

Figure 1: Slots available for the addition of cryomodules

2.2 Cavity

For the CEBAF accelerator to reach 12 GeV, the Upgrade Cryomodules will be required to supply an average energy gain of 68 MeV.[5] This will be accomplished by an increase in both the operating gradient and the active length of the cryomodule. An increase in active length from 4 m to 5.6 m must be accomplished within the

* Work supported by the U.S. DOE. Contract # DE-AC05-84ER40150
# E-mail: delayen@jlab.org

existing cryomodule footprint. The increased active length and an average operating accelerating gradient of 12.5 MV/m provide the required energy gain from a cryomodule. To operate at this gradient within the planned 2 K refrigeration capacity, the quality factor of the cavities must be maintained at 6.5×10^9 or above.

2.3 Fundamental Power Coupling

The Upgrade Cryomodule will be operated with the existing 5 kW RF power sources upgraded to 6 kW. The fundamental power coupler (FPC) is designed to use a minimum of RF power for gradient and phase control. The nominal fundamental power coupler Q_{ext} is 2.2×10^7.[6,7] To support cavity-to-cavity alignment in the cavity string, an additional requirement for the coupler is insensitivity to mechanical deformation of 0.0013 m axially and 0.050 rad angularly.

2.4 Helium Vessel

The helium vessel encloses the cavity cells only, minimizing the liquid helium inventory in the cryomodule. This is a change from the existing CEBAF design that encloses the FPC and the HOM coupler ports. The vessel design uses titanium construction with two titanium bellows at the outer diameter.

2.5 Beamline Interface

The beamline between cavities became crowded as efforts to maximize the active length of the cryomodule progressed. The decision was made to remove all bellows between cavities, allowing two additional cells, or 0.20 m active length per cavity. The beamline outside the helium vessel contains the higher-order-mode (HOM) coupler ports, fundamental power coupler, field probe port, and frequency tuner attachment.

2.6 Tuning

The baseline tuning system design includes a coarse and fine tuning actuator. This is a change from the existing CEBAF design that has a single tuning actuator. Fine tuning is needed to minimize the RF power required. A control resolution of 1 Hz with a range of +/- 1 kHz is required for the fine tuner, and a resolution of 100 Hz with a range of 400 kHz is required for the coarse tuner.[8] The range of the fine tuner is sufficient to handle the normal operating requirements, which are typically within 100 Hz, while the coarse tuner is used to tune the cavities after cooldown, or when additional range is required. Simpler designs that may meet the requirements are also under investigation.

2.7 Cavity Suspension and Alignment

The cavity alignment requirements are unchanged from the original CEBAF requirements.[9,10] Cavities must be aligned relative to the nominal beam trajectory with an rms angular precision of 0.002 rad. To accomplish this, a space frame will be constructed around the completed cavity string that will allow individual cavities to be final-aligned in the as-installed support configuration.

2.8 Microphonics, RF Control, and RF Power

To contain cost, we have adopted as a goal only a modest increase of the RF power per cavity from 5 to 6 kW. This puts stringent requirements on microphonics and the control system. At 12.5 MV/m and 400 μA circulating current, the maximum allowable amount of detuning (including static and microphonics) is 25 Hz. The optimum Q_{ext} is 2.2×10^7, and the Lorentz detuning is much larger than the loaded bandwidth; for this reason a new low-level RF control system will be required. The baseline concept is an agile digital system capable of implementing a self-excited loop on I/Q feedback.[11]

2.9 Requirements Summary

Many of the requirements for the Upgrade Cryomodule are very similar to those for the original CEBAF cryomodule. This results from maintaining the existing half-cell slot footprint. Differences in the Upgrade Cryomodule and the original cryomodule are primarily driven by the increased energy gain, improvements in fabrication techniques, and changes in beam requirements. Table 1 contrasts linac cryomodules for the original 4 GeV CEBAF with linac cryomodules for the envisioned 12 GeV CEBAF upgrade.

3 CAVITIES

3.1 Introduction

To increase the voltage from a cryomodule requires increasing the cavity-operating gradient, or increasing the effective accelerating length, or both. Maximizing the accelerating length is arguably the approach that presents the least technological risk. In any case, for CW accelerators such as CEBAF, maximizing the length instead of the gradient has the clear advantage of lowering the dynamic load on the refrigeration system.

For this reason, it was decided early that the Upgrade Cryomodule would still include eight cavities, but that these would be of a seven-cell (70 cm) design instead of the present five-cell (50 cm) design. The requirement described in Section 4.2.2 calls for these cavities to provide a minimum voltage of 8.75 MV with a maximum power dissipation of 17.5 W; i.e., their Q must be at least 6.5×10^9 at 12.5 MV/m. Thus the greatest challenge is not so much achieving a high gradient as maintaining a high Q at high gradient. Given the constraint imposed by the available refrigeration, CW operation at 15 MV/m would be practical only if the Q at that field were at least 10^{10}. See Figure 2.

Table 1: Linac Cryomodules: 4 GeV CEBAF vs. 12 GeV CEBAF

Parameter	Linac CMs for 4 GeV	Linac CMs for 12 GeV	
	Original	Retained original	Upgrade
Acceleration	400 MeV	544 MeV	546 MeV
Maximum linac current	1000 μA	430 μA	430 μA
Linac slot length	9.6 m	9.6 m	9.6 m
CM slot length	8.25 m	8.25 m	8.71 m
Warm vac. slot length	1.35 m	1.35 m (also 1.12 m)	0.89 m
# CM/linac	20	17	8
Voltage/CM	20 MV	32 MV	68 MV
E_{acc} Average	5 MV/m	8 MV/m	12.2 MV/m
Q_0 @ E_{acc}	2.4×10^9	5.0×10^9	6.5×10^9
RF windows	2	same	1
FPC coupling	λ/2 stub on stub	same	λ/4 stub
Q_{ext} FPC	6.6×10^6	same	2.2×10^7
HOM coupling	Waveguide	same	Coaxial
B.L. bellows	5	same	2
Vac. valves	10	same	4
Freq. tuner	Single	same	Dual (coarse/fine)
Cryounits (CU)	4	same	1
Cavities/CU	2	same	8
2 K RF heat load	45 W	72 W	160 W
50 K RF heat load	20 W	40 W	120 W
2 K Static heat load	15 W	15 W	25 W
50 K static heat load	140 W	140 W	180 W

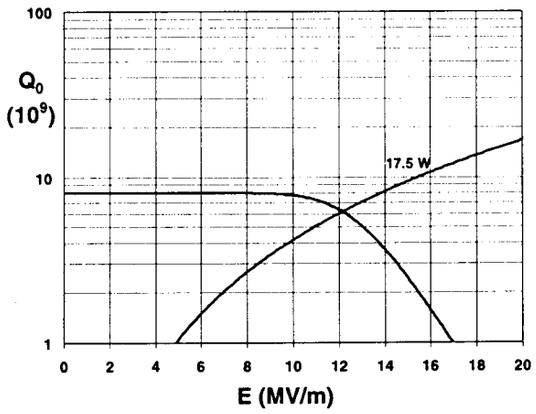

Figure 2: Design Q-curve for the upgrade seven-cell cavity, with line of constant 17.5 W power dissipation

3.2 Cell Geometry

While the CEBAF cavity cell design could be improved, the potential benefits do not seem critically important, and the first seven-cell cavity prototype has been built using the existing cell design and has met the requirement of a Q of 6.5×10^9 at 12.5 MV/m.[12]

The existing cell shape is characterized by ratios E_p/E_{acc} of 2.6 and H_p/E_{acc} of 47 Oe/(MV/m). Designs with lower ratios exist; however, as was mentioned before, the greatest challenge is not so much high gradient as low power dissipation. In that respect, the shunt impedance of the existing design compares well with that of others. Another attractive feature of the existing cell design is the relatively high cell-to-cell coupling coefficient (3.3%), which reduces the sensitivity of the field profile to mechanical tolerances and mechanical stability as the number of cells is increased. A redesign of the cells is still an option, although a low-priority one.

3.3 Intercavity Beamline

The topology of the Upgrade Cryomodule places a full complement of couplers between each pair of adjacent cavities. The mechanical design of this region has proved to be a challenge. The required functionality includes: a fundamental power coupler (FPC), two coaxial higher-order-mode (HOM) dampers, a field probe, the tuner, connections to the LHe vessel, and a demountable joint.
A concern raised in seeking longer accelerating length within the same overall cryomodule footprint (increasing fill factor) is that the separation between cavities could

prove to be small enough to lead to undesirable amounts of cross talk. This was explored at some length [13] and found not to be a problem. For very short separations, half-integral wavelength separations ($\lambda/2$, or λ) are needed to keep the real power flow small. $\lambda/2$ spacing is much too short to allow placing couplers in the intercavity space, and would mean severe demands on the demountable joint. λ spacing has some attractive features, and some attempts were made to design the needed functionality into this space. No solutions were found that appeared practical to assemble.

For separations larger than λ, the cross talk between adjacent cavities is small enough not to require a "magic" choice of distance. At the current design value of 30 cm (1.5 λ), the power flow between cavities under nominal conditions is negligible.[13]

3.4 Fundamental Power Coupler

Experience with waveguide couplers in the CEBAF design was generally positive. Waveguide couplers can be made relatively flexible and forgiving of displacements along the beamline. Heat loads are easily controlled, and there are no tight manufacturing tolerances. Waveguide couplers are also relatively inexpensive compared to coaxial couplers.

One unpleasant feature of the original waveguide coupler was a large transverse beam kick. This characteristic originated from its storage ring heritage, where the damping of the $4\pi/5$ TM_{010} mode was important for beam stability. In the present (relatively) low-current linac application, this is not an issue, and the coupler itself could be adjusted for near zero transverse kick.[6]

Another feature in our existing coupler system where improvements could be made is related to the windows, in particular the location of the cold window close to the beamline. We have settled on a revised topology [7] that has a single warm ceramic window, shielded from line-of-sight interaction with the cold cavity, that is not required to pass HOMs. This does place more stringent demands on the waveguide thermal transition. It must be installed nearly free of particulates and have low outgassing characteristics.

The fundamental power coupler is of the waveguide type and has been designed and tested using a copper model. The coupler uses a $\lambda/4$ stub geometry providing two significant benefits: minimization of steering kicks resulting from the coupler electric fields and insensitivity to minor mechanical deformations in the coupler. The first is important to minimize the effects on the beam quality in the accelerator, while the second allows for using the coupler for small cavity alignment adjustments. A copper coupler model has been used to determine final dimensions and demonstrate the required tolerance to mechanical deformations.

In order to minimize the required RF power at the design gradient and circulating current a cavity-coupling factor was chosen to be 2.2×10^7 (Figure 3). A $\lambda/4$ stub waveguide coupler intersecting the beampipe couples the TE_{01} waveguide mode to the evanescent TM_{01} cavity mode. The waveguide-coupler-to-cavity separation was selected to achieve the desired coupling.

The Cornell/CEBAF cavity currently used has a $\lambda/2$ stub waveguide coupler and was originally designed for storage ring applications. In the Cornell storage ring the $\lambda/2$ stub coupler provided a Q_{ext} of 3×10^5 and was located up against the iris of an end cell. For use in CEBAF, the Q_{ext} was increased to 6×10^6 by changing the stub length, leaving the coupler-to-end-cell distance unchanged. Coupling to the fundamental can occur with the stub length slightly less than $\lambda/2$, while TE_{111} cavity modes in the 1.7 to 1.9 GHz range, which are beyond cut-off of the waveguide HOM couplers, are even more strongly damped. This feature is not relevant for the energy upgrade cavity, which will have coaxial HOM dampers. Furthermore, there are several disadvantages to the $\lambda/2$ coupler over the $\lambda/4$ coupler. Locating the beamline close to the null in the standing wave pattern makes the coupler Q_{ext} quite sensitive to small shifts in this pattern due to manufacturing tolerances and subsequent waveguide deformations. This becomes even more acute for the higher fundamental rejection required for Q_{ext} of 2.2×10^7 as opposed to 3×10^5. Another drawback is the field asymmetry across the beampipe that gives rise to a "coupler kick". In CEBAF this effect was reduced by alternating the longitudinal coupler orientation in a pattern averaging the net kick to an acceptable level. [6,14]

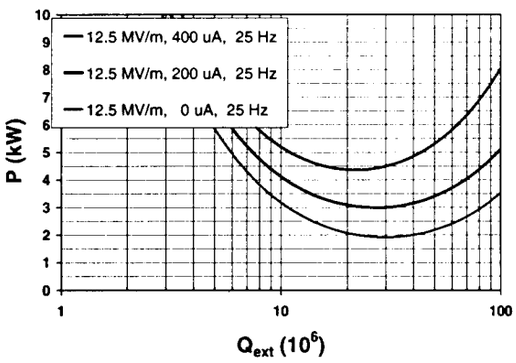

Figure 3: Required RF power as a function of Q_{ext} at 12.5 MV/m and total detuning of 25 Hz for circulating currents of 0, 200, and 400 μA

Figure 4 shows the electric field in the centerline of the $\lambda/2$ stub of the CEBAF cavity. The curve labeled "Real" is

the component of a travelling wave that is in phase with the evanescent fields in the beampipe. It is also the standing wave pattern when the cavity is filled, as would occur in steady state on resonance. The curve labeled "Imag" is the component of a travelling wave that is in quadrature with the evanescent fields in the beampipe. It is also the standing wave pattern when the cavity is empty, as would occur off resonance. Fields in the stub reach 14 times the peak field in the unperturbed waveguide. The resulting heat deposited in the FPC body would be problematic in designs with the FPC outside the helium vessel.

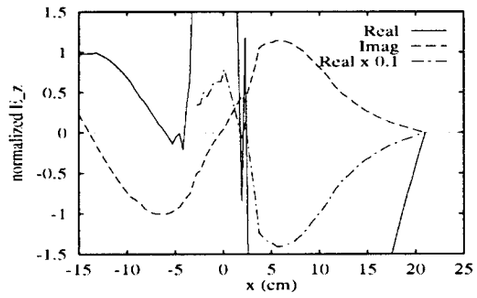

Figure 4: Electric fields in the centerline of λ/2 stub-on-stub PC used by the Cornell/JLab cavity system. [3]

In order to overcome all these limitations, a λ/4 stub waveguide coupler was chosen for the 7-cell energy upgrade cavity. Figure 5 shows the electric field along the FPC waveguide centered on the beam line for this configuration. [6] In addition to eliminating the "coupler kick," the coupler fields are much reduced and will contribute negligible heat to the coupler body outside the helium envelope.

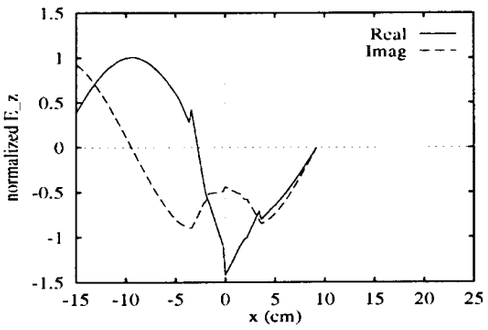

Figure 5: Electric fields in the centerline of λ/4 stub fundamental power coupler proposed for the CEBAF energy upgrade cryomodule. [6]

The sensitivity of Q_{ext} of the FPC to mechanical deformation and variations in manufacturing tolerances has also been reduced significantly. We have used this insensitivity by allowing the FPC waveguide to take up cavity misalignment and axial beam line displacement without significant change in the cavity coupling factor. The Q_{ext} variation with axial deformation (i.e., reducing or increasing the height of the FPC waveguide at the beampipe) is 6%/mm for small displacements. For angular displacements of the beampipe away from the beamline, rotating about the center of the FPC waveguide, the Q_{ext} variation is 0.15%/mrad. Consequently, the beamline between cavities could be made entirely niobium, with no bellows. Some flexibility has also been included in the niobium flanges joining cavities. A combination of trimming cavity length plus these two flexible elements is used to absorb all misalignment and length variation in the beamline.

3.5 Higher-Order-Mode Couplers

Among the modifications to be implemented in the cavities is the HOM damping scheme. In the original CEBAF design, a healthy safety factor against multipass beam breakup (BBU) was included. The Q's of the relevant dipole modes were maintained at the 10^3–10^4 level in order to guarantee two orders of magnitude margin in the threshold current for instability. To re-evaluate the requirements for HOM damping in CEBAF, a program of measurements, simulations and experiments is being implemented. Measurements of HOMs in the accelerator and FEL have shown that self-polarization of the coupler can enhance the Q of some modes to levels as high as 5×10^7. Even with these high Q's the machine is stable against BBU for the nominal current. Therefore we expect that, for the upgrade, even higher Q_{ext} would be acceptable because the average current in the accelerator will be lower, and the injection energy and the overall energy of CEBAF will be higher. We estimate that the requirements on the Q_{ext} of dipole modes could be relaxed by about two orders of magnitude, up to 10^5-10^6 from 10^3-10^4.

At present, the baseline design includes a tuned filter HOM damping scheme following the TESLA-Saclay design [15], which is compatible with the integrated helium vessel used for the upgrade cavities.

The possibility of eliminating entirely specialized HOM absorbers is also under investigation. A program of studies of HOMs is being implemented which will help in clarifying the true HOM limitations at CEBAF and in the FEL.

3.6 Prototype Seven-Cell Cavity

A seven-cell cavity was built from existing half-cells and dumbbells remaining from the CEBAF cavity production phase (Figure 6). Particular care was taken in the preparation of the dumbbells prior to joining them by

electron beam welding. Each dumbbell was carefully inspected and mechanically ground, removing all visible surface imperfections such as indentations or scratches.

Subsequently, the dumbbells were degreased and chemically polished for 1–2 min, partially removing the surface damage layer. The equatorial welds were done from the outside with standard welding parameters, but only one dumbbell was added at a time, starting from one end half-cell, and each weld was thoroughly inspected. If necessary, some mechanical grinding of the welds was done with subsequent degreasing and slight chemical polishing. Prior to completing the equatorial welds, beampipe assemblies were welded to the end half-cells.

Figure 6: Prototype seven-cell cavity prior to the welding of the titanium tank.

The cavity had a π-mode frequency of 1494.45 MHz with a field-unflatness of 16% (in E^2). After pre-tuning the π-mode to 1494.6 MHz and a field flatness of 5%, the cavity was chemically pre-polished three times for a total of 7.5 min; the acid temperature did not rise above 25 °C. The total frequency shift was about −500 kHz, corresponding to a material removal of approximately 90 μm, assuming a uniform material removal over the entire cavity surface.

For the final surface preparation, the cavity was degreased for 1 hour in a caustic solution with ultrasonic agitation. After pure water rinsing, buffered chemical polishing removed an additional 75 μm. Thorough rinsing was followed by high-pressure ultrapure water rinsing for more than 90 min.

In the clean room the cavity was rinsed twice with reagent grade methanol. Immediately after assembly, the cavity was attached to the vertical test stand and evacuated by a turbo pump for typically 15 min. When a pressure of less than 5×10^{-6} torr was reached at the turbo pump, the cavity vacuum system was transferred to the ion pump on the test stand. Fast cooldown of the cavity to 4.2 K took place in approximately 1 hour; during pump-down to 2 K the temperature dependence of the surface resistance was measured. A residual surface resistance of 7.8 nΩ corresponding to a Q_{res} of 3.5×10^{11} was measured.

At 2 K the cavity gradient was initially limited to 16.3 MV/m by a breakdown, which seemed to be initiated by field emission. After He-processing the quench limit improved to 17.5 MV/m at a Q-value of 6.2×10^9 (Figure 4.3-6). During the pump-down of the helium bath from 4.2 K to 2 K, a pressure sensitivity of 99 Hz/torr was measured.

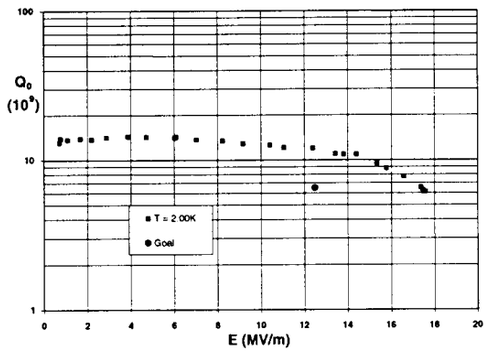

Figure 7: Results of the test of the first seven-cell prototype

4 CRYOMODULE

4.1 Concept

The existing CEBAF cryomodule is constructed from four cryounits, each containing a sealed cavity pair. These cryounits are then joined with bridging sections. In order to increase the number of cells from five to seven while maintaining the same cryomodule length, this approach had to be abandoned. [5,16]

Several cryostat concepts were explored:

- Cylindrical cryostat with radial penetrations for the power couplers.
- Cylindrical cryostat with axial (through the end plates) penetrations.
- Bathtub-type cryostat where all the innards are suspended from a top plate.

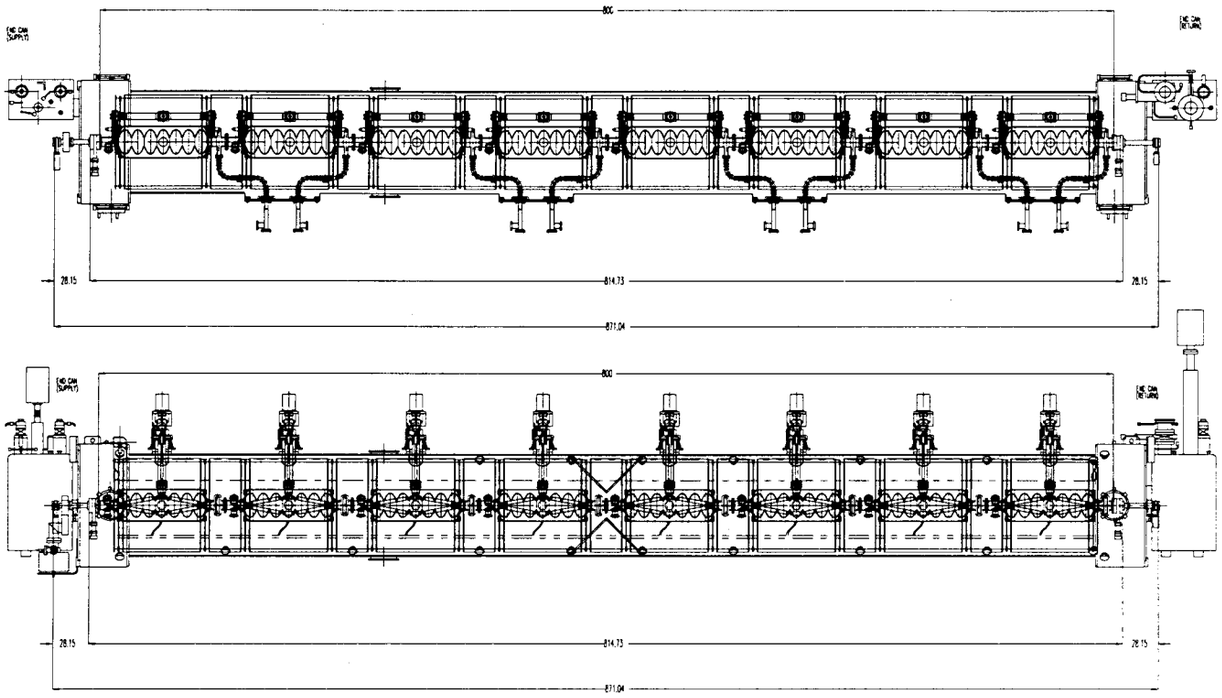

Figure 8: Top and side view of the Upgrade Cryomodule (cm)

While all designs had advantages and disadvantages, a cost/benefit analysis did not reveal an obviously preferred option. The overriding consideration was the limited amount of time and resources expected to be available. The radial design was chosen as it was deemed the one that would require the least amount of development given the on-site experience with this concept.

The Upgrade Cryomodule will include a continuous eight-cavity string assembly without isolation valves between the cavities. The present design calls for a 30 cm separation between cavities into which must fit the fundamental power coupler, the higher-mode extraction system, the pickup probe, connecting flanges and connections to the helium tank and mechanical tuners. The design does not include bellows between the cavities.

The overall concept for the cryomodule is shown in Figures 8, 9, and 10.

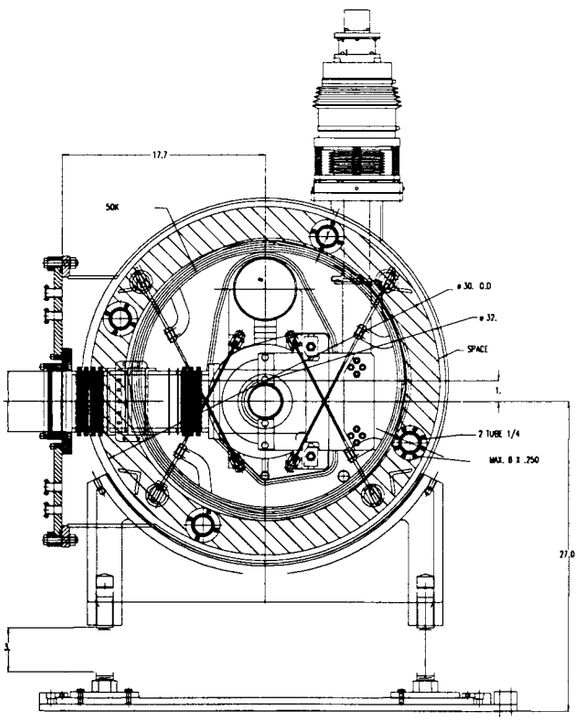

Figure 9: Cross-section of the cryomodule

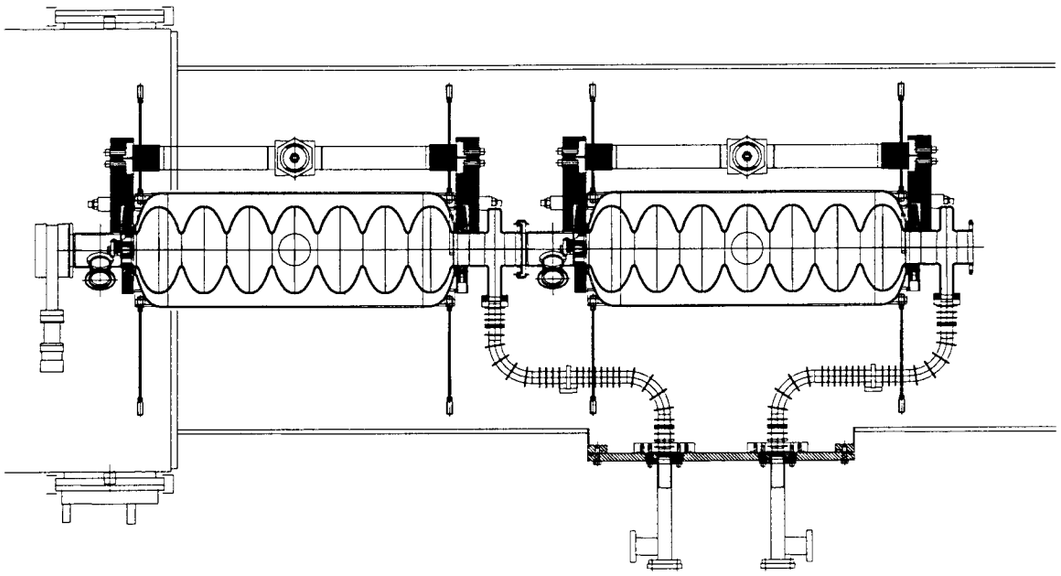

Figure 10: Detail of the beamline layout at the end of the Upgrade Cryomodule

4.2 Cavity

The cavity assembly has seven cells using the CEBAF cell designs for interior and end cells. The cells are assembled with an end collar that provides the interface to the helium vessel, beamline, and tuner attachment. A major difference from the original CEBAF design is the use of a single eight-cavity hermetic sealed string replacing the four hermetic cavity pairs.

4.3 Fundamental Power Coupler

The nominal cavity gradient is 12.5 MV/m with a beam current of 430 μA. A shorted waveguide intercepting the beampipe couples RF power to the evanescent TM_{010} mode of a seven-cell cavity (Figure 11). A copper-plated stainless steel waveguide provides a thermal transition between the cavity at 2 K and the outer cryostat envelope at 300 K. The cavity vacuum extends to a single rectangular waveguide window at 300 K.

The new beamline configuration reflects several changes. With no gate-valves or bellows between cavities, cavity length increased from five to seven cells. This requires both lateral and radial flexibility in the waveguide thermal transition to allow for thermal differential contraction between the cavity string and the outer vacuum envelope, the accumulated cavity motion arising from cavity tuner operation, and manufacturing tolerances. The longitudinal motion of the string of eight cavities will be fixed at the center of the cryomodule requiring a displacement at each end amounting to 1.6 cm. Three short waveguide bellows appropriately placed provide this motion.

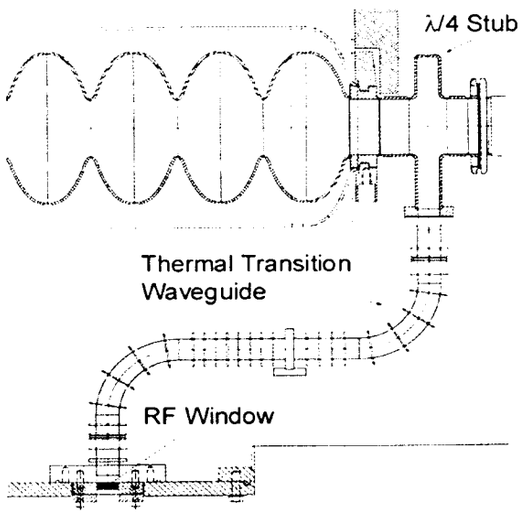

Figure 11: Cavity-waveguide-coupler system

The cavities' flexible waveguides and warm windows are attached in the clean room, with the entire cavity string then permanently evacuated for all subsequent cryomodule assembly. As shown, each waveguide has two 90° elbows. This accomplishes two purposes:

reduction of radial penetration ports from eight to four, and avoidance of window charging leading to arc trips by removing the ceramic window from the field-emitted electrons and the radiation flux. Currently 40% of CEBAF cavities are limited in gradient by field-emission-induced arcing. Tests have shown that moving the RF window from a direct line-of-sight view of the high-field region of the cavity can eliminate field-emission-induced window arcs. The need to offset the window to prevent arcing and the need for longitudinal motion were factors favoring the simplicity of a waveguide coupler over a coaxial design.

The waveguide section that provides the thermal transition between the cavity and vacuum vessel has a common vacuum with the cavity and is sealed with a warm ceramic window. The waveguide incorporates an S-bend which allows for the grouping of waveguides in pairs prior to penetrating the vacuum vessel and removes the warm ceramic window from the line of sight of the beamline.

A copper-plated stainless steel waveguide provides the required thermal isolation between an RF window at 300 K and the cavity waveguide coupler flange at 2 K, with thermal intercepts at 40 and 60 K (via different thermal strap lengths to 40 K shield). The FPC refrigeration load at 2 K is the sum of thermal conduction and RF dissipation from the waveguide between 2 K and 50 K, and is minimized, for a given waveguide structure, with respect to waveguide length.

The RF fields averaged circumferentially over a slice of waveguide perpendicular to the direction of propagation are shown in Figure 12 for normal operating conditions and in Figure 13 for the worst-case condition.[17]

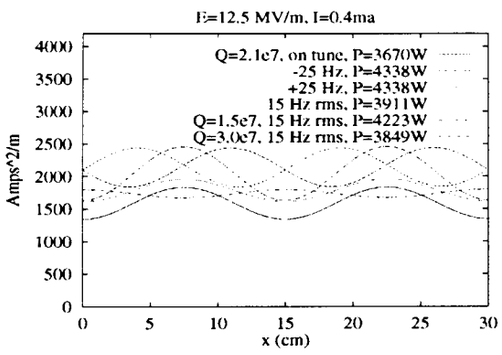

Figure 12: Typical currents on waveguide walls [17]

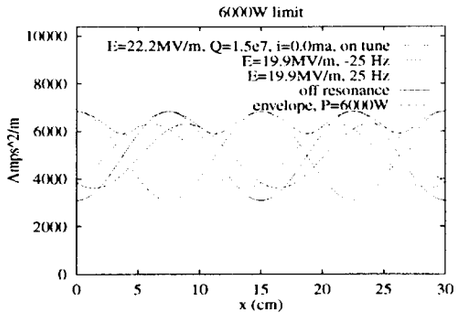

Figure 13: Worst-case current on waveguide walls [17]

In balancing RF dissipation against heat conduction down the guide, a broad minimum in 2 K heat load as a function of waveguide length is seen (Figure 14).

When operated at a minimum, the highest temperature along the waveguide will be at the high temperature end of the guide. Under worst-case conditions the same waveguide will reach a peak temperature somewhere along the guide significantly higher than the end of the guide. The potential for sudden gas migration in such an excursion possibly inducing waveguide discharge will be studied with prototype components in a horizontal test cryostat later this year. Details of the copper plating will also be studied.

The heat load at 2 K will be less than 1 W under normal operating conditions. The minimum length-optimized heat load will depend on the total thermal conductance of the stainless steel waveguide walls and of the copper plating in addition to the RF loss in the copper. Although the surface impedance of the copper is predominantly in the anomalous limit between 2 K and 50 K, the residual resistivity ratio (RRR) and thickness of the copper layer have a significant influence, and must be chosen to balance performance risk against overly conservative manufacturing tolerances. [18]

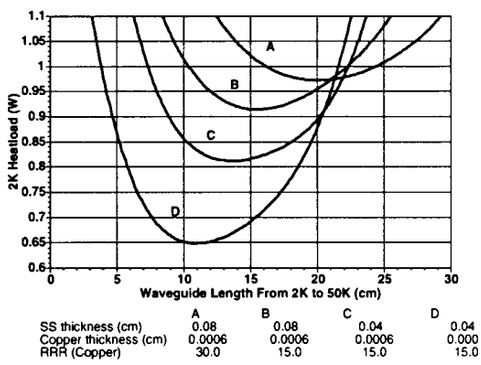

Figure 14: Heat load along the waveguide as a function of waveguide length between 2 and 50 K

Each coupler contains one RF window at 300 K. The window is a thin metal-ceramic waveguide window using a rectangular copper-gasketed knife-edge seal on the cavity vacuum side. A variety of similar windows have been developed at JLab having RF power-handling capabilities in excess of the CEBAF energy upgrade requirements. The VSWR is less than 1.1 to 1 through the use of compensating irises built into the window.

Other designs incorporating straight waveguide sections are also under investigation. These would be better optimized for higher power applications (higher gradient and/or higher current) and might be easier to manufacture.

4.4 Beamline

The beamline is the area outside the helium vessel and includes the FPC, HOM coupler ports, field probe, beamline flanges, and tuner attachment points (Figure 15). Noticeably missing between the cavities are any bellows or vacuum valves. To allow for the lack of beamline bellows, the beamline flanges and FPC must provide the adjustment required to maintain cavity alignment. Additionally, trimming the stub ends allows for adjusting the overall cavity length to compensate for the lack of in-line bellows. Adjustment on the helium vessel is achieved through additional stroke on the bellows and vessel welding.

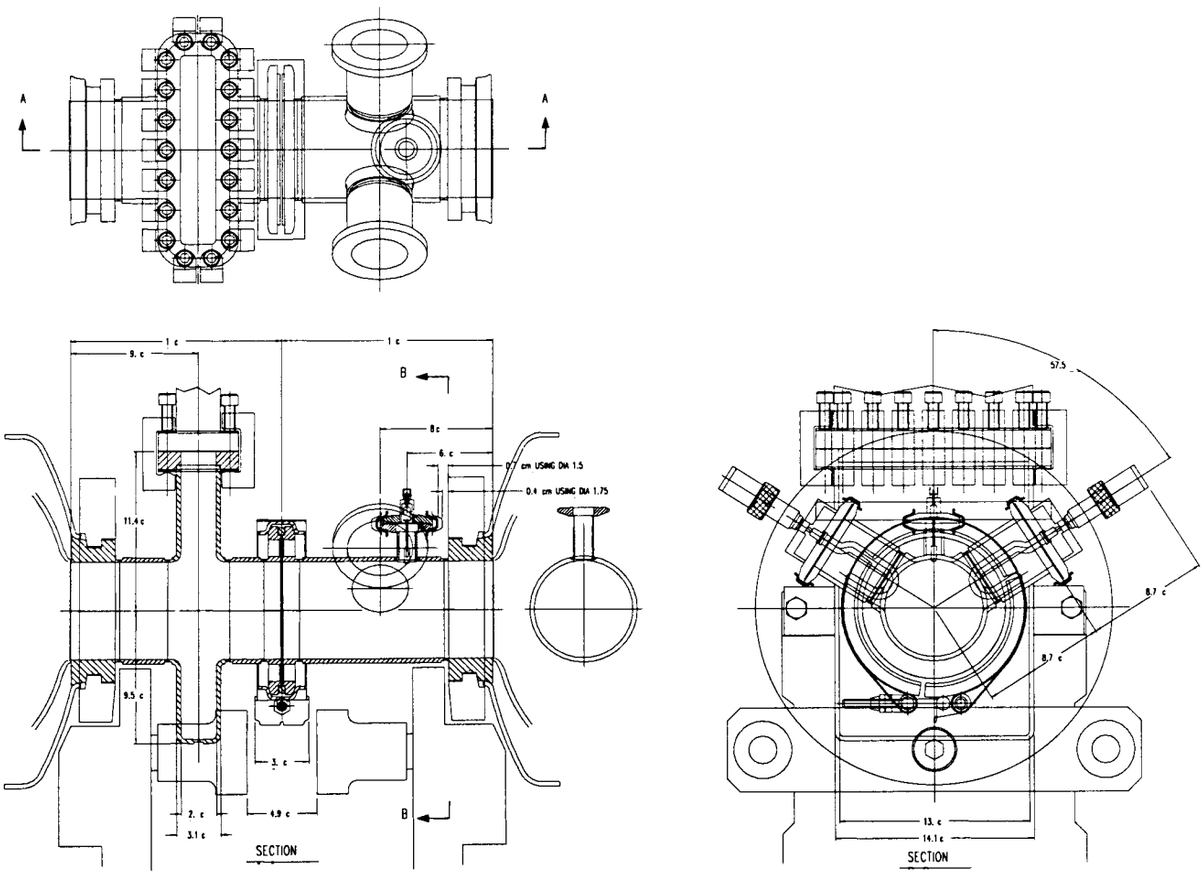

Figure 15: Detail of the beamline region between two cavities

The beamline flanges allow for an angular deflection by utilizing a design that thins the material interior to the sealing surface. Deformation of the membrane results in the required angular deflection. The FPC provides additional axial and angular deflection where the beamline tube intersects the waveguide box. The combination of these allows for a dogleg displacement in the beamline.

4.5 Helium Vessel

The helium vessel is one of the major changes from the CEBAF design. The vessel has been reduced from a 0.61 m to a 0.25 m diameter. This is made possible by moving the RF couplers and tuner assembly outside of the helium vessel. The vessel material is titanium to match the thermal properties of the cavities and minimize differential thermal contraction difficulties. Two titanium bellows are incorporated into the vessel which allow for the remaining differential thermal contraction and tuning requirements.

4.6 Cavity Frequency Tuning

The cavities in the CEBAF Upgrade Cryomodule will differ from the existing ones in several respects: they will be 40% longer (seven-cell instead of five-cell) and have a design gradient of 12.5 MV/m instead of 5 MV/m. In spite of their having an energy content seven times larger at design field, we have adopted as a goal only a modest increase of the RF power per cavity from 5 to 6 kW.

As shown in Figure 16, in order to operate at 12.5 MV/m with a circulating current of 400 μA, the total amount of detuning, both static (average frequency offset) and dynamic (microphonics) must not exceed 25 Hz. This would give sufficient margin for RF control and allow for errors in the external coupling. For this reason, the frequency tuner will be required to achieve a frequency resolution of 1 Hz. Because the needed resolution is much less than the Lorentz detuning (~ 500 Hz) and the sensitivity to pressure fluctuations (~ 100 Hz/torr), the cavity frequency may need to be adjusted frequently without impact on operation. It is unlikely that a pure mechanical tuner, similar to the one in use at CEBAF, would fulfill the requirements because of the associated vibration, deadband, backlash, and non-monotonicity.

On the other hand, the tuning range must be adequate (+/- 200 kHz) to compensate for variability in manufacturing, chemical processing, and cooldown, and to allow for substantial detuning of cavities that are not operating.

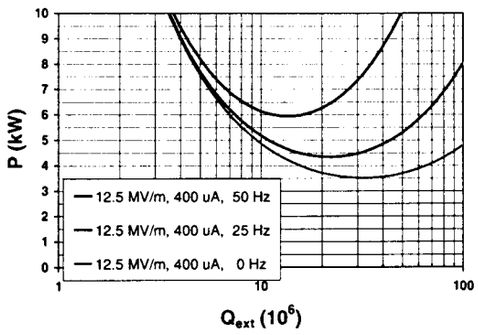

Figure 16: Required RF power vs. external Q at the design gradient of 12.5 MV/m, design current of 400 μA, and maximum detuning of 0, 25, and 50 Hz

In order to satisfy these requirements, the tuning system, shown in Figures 17, 18, and 19, has been divided into two parts: a coarse tuner with a range of +/- 200 kHz and resolution of 100 Hz, that is expected to be used infrequently; and a fine tuner with a range of +/- 1 kHz and resolution of 1 Hz that will be used during normal operation.

The fine tuner makes use of piezoelectric actuators to avoid the friction on mechanical components that would otherwise adversely affect the resolution and the life expectancy of the mechanism. The fine tuner can therefore be used for continuous small corrections to the cavity frequency, over its range of +/- 1 kHz. The coarse tune adjustment of +/- 200 kHz is actuated by a stepping motor through a harmonic drive reducer and a ball screw. Both systems are external to the vacuum enclosure, and are at ambient temperature and therefore accessible for maintenance and repair. The tuning motion of either drive system is brought into the cryostat through two thin-wall concentric tubes (Items 1 and 2, Fig.17), both moving axially and relative to one another. From that linear motion feedthrough, all other tuning motion is generated using metal flex joints only. The tubes are connected respectively to the upper and lower arms (Item 3 and 4, Fig. 17 of a scissors-type jack. In this way the motion of the tubes translates into a linear stroke parallel to the cavity centerline. Installation of the tuner actuator outside the vacuum vessel is offset relative to the cavity and scissors jack warm position. This offset compensates for the cavity movement resulting from thermal contraction and places the tuner actuator in proper alignment with the scissors jack during normal operation.

The niobium cavity (Item 5, Figure 18) as two reinforcing and attachment rings (Item 6), one on each end of the seven-cell array, with each having a wedge-shaped groove machined into its outside surface for positive attachment points. There is a split-ring clamp (Item 7) engaging each of these that is used to mount the tuner. Titanium flex inserts (Item 8) connect the split rings to two pivot plates (Item 9), one on each end of the cavity. At the midpoint of these plates, two compression bars (Item 10, Figure 17 extend from one plate parallel to the cavity centerline to the other plate, providing fulcrum points for both pivot plates. Titanium flex inserts again are used at the connecting points of this arrangement. The other end of each of these pivot plates is fastened to the above-described scissors-type jacks, again using flex inserts, to complete the power train of the system. The cavities are manufactured and tuned to achieve their nominal frequency when extended by 0.75 mm, so that the tuner components are in tension at all times, in order to provide a backlash-free tuning range. The fine tuning actuators are three piezoelectric post type units (Item 11, Fig. 19) located between the upper and lower mounting plates (Items 12 and 13). They are spaced uniformly around the ball screw nut (Item 14) and work in compression only. They are low voltage units (150 VDC) with a stroke of 50 μm. The scissors jack, pivot plates, and split rings are machined from 6AL/4V titanium, which has similar coefficient of thermal expansion to niobium. The thrust tubes are made of type 304 stainless steel and have thin wall areas to minimize thermal conduction to the cavities. The baseline tuner design is complete and a prototype is being fabricated for testing in the Horizontal Test Bed described in subsection 4.9. Other purely mechanical options are also being investigated since, if it can be demonstrated that they can fulfill our requirements, they would be more cost-effective.

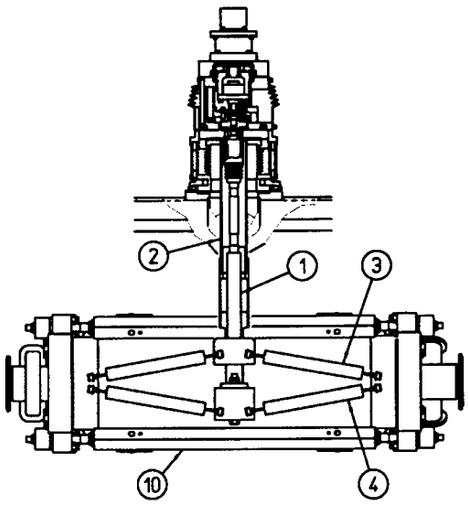

Figure 17: Scissors type jack

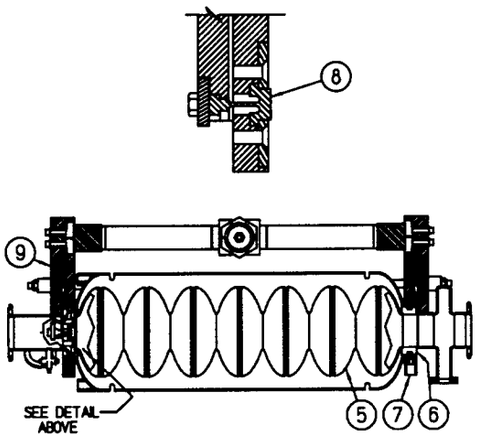

Figure 18: Pivot plate arrangement

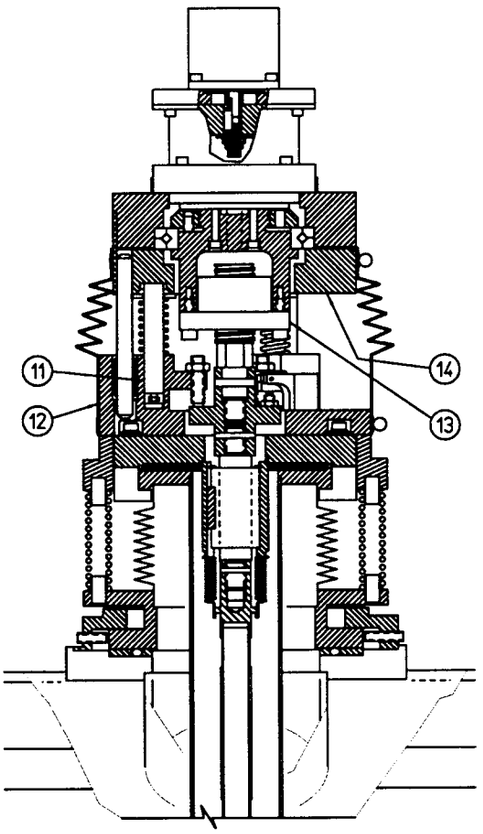

Figure 19: Tuner drive assembly

4.7 Support and Alignment

A warm space frame using support rods configured in a double-paired cross pattern at each end supports each

cavity in the cavity string. The space frame is supported inside the vacuum vessel at the quarter points, each being between the second and third cavity from the end. The frame is made up of a series of hoop rings installed perpendicular to the beam axis down the length of the cavity string and connected by axial support members. The frame is assembled around the string along with the tuner assemblies starting from one end and progressing to the other. When the space frame is completed, magnetic shielding, thermal shielding, and associated components will be added to the structure. When complete, the space frame will be wheeled into the vacuum vessel and locked into position. The space frame concept is shown in Figure 20.

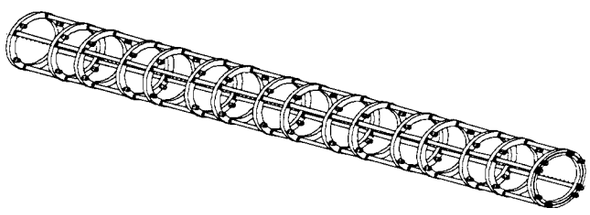

Figure 20: Concept of the space frame for support and alignment of the cavity string.

4.8 Vacuum Vessel

The vacuum vessel is designed as a single pipe running the length of the cavity string. Four horizontal penetrations allow for bringing the waveguides and instrumentation out of the vacuum vessel. Eight smaller penetrations on the top of the cryostat allow for the tuner interface.

4.9 Testing

The Upgrade Cryomodule includes new design concepts for several components. A testing program has been designed to validate these concepts early on, providing confidence for the continuing design effort. A facility is under construction to provide a means to test various components. An important feature of this facility is the ability to quickly install, test, and remove components, allowing for multiple tests in a short period of time. This facility, the Horizontal Test Bed (HTB) shown in Figure 21, is being fabricated by modifying an early CEBAF prototype cryounit. The HTB will allow for the testing of two cavities with prototype components attached. Its commissioning is planned for fall 1999, and the first test with prototype components for a single cavity is scheduled for December 1999.

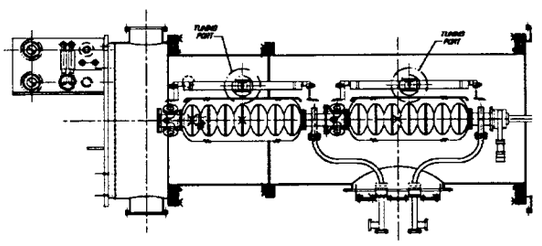

Figure 21: Horizontal Test Bed for the tuner, coupler, and cavity prototypes

4.10 Design Integration

The design of the cryomodule includes many closely interacting components. An attempt has been made to optimize critical high-impact systems as a whole with regard to these interactions. This has necessitated a number of iterations in design as one component design evolves and the resulting impact on others is evaluated and considered. The beamline area has been the focus of considerable effort to date. This area includes all the RF coupling, the tuner attachment, and cavity support and alignment. The important issues include space, performance, fabrication, and processing considerations.

5 FACILITY UPGRADES AND PROCEDURES

5.1 Facility Upgrades and Procedures

To meet the design specification of high gradients and low losses with tighter distribution in performance, and to provide for mechanical changes to the cavity and cryostat design, we concluded that an upgrade of the facilities and of the assembly procedures used previously for the fabrication of CEBAF cryomodules was needed. The goal was to increase the control over process and assembly variables.

The production run of CEBAF cryomodules (1990–1994) generated a broad distribution of acceptable operating gradients between 4 and 14 MV/m. The predominant limitation in individual cavity performance is field emission and field-emission-related RF window arcing, mainly due to surface contamination from process and hardware particulates. Our review has led to an assembly procedure that will pre-qualify the seven-cell cavities by vertical testing of the seven-cell assembly prior to addition of beam tube couplers. After qualification, the couplers and helium vessel will be added and the cavity will be prepared for final assembly of an eight-cavity string. The final string assembly will then be completed

in the Class 100 production clean room. To reduce particulates and to narrow the individual cavity performances in the final string, production semiconductor-style chemistry and high-pressure-rinsing (HPR) cabinets have been installed in the clean room (Figure 22). The chemistry and the HPR cabinets are self-contained, PLC-controlled and menu-driven. In addition to these cabinets, a part-cleaning cabinet and a final ozone-rinsing cabinet are currently being designed for use in part of the final string assembly procedures. During the commissioning of these new facilities, procedures will be adjusted as necessary to reduce exposure of internal cavity surfaces to particulates generated by assembly in order to meet the new module performance specifications.

Figure 22: Closed chemistry cabinet (right) and high-pressure rinsing cabinet (left) in the Class 100 production clean room during shutdown for installation.

5.2 Tooling

Tooling is being developed for the seven-cell cavity processing, full cavity fabrication, cavity string assembly, and cryomodule assembly. Cavity handling tooling has been designed and, whenever possible, is compatible with the existing cavity tooling. Integrated functionality tooling handles seven-cell cavity processing in the clean room, assembly of full cavity with beamlines and helium vessel, welding fixturing for the e-beam welder, and cavity string assembly in the clean room. Such tooling is shown in Figure 23. Cryomodule assembly tooling is still being developed which will utilize the existing assembly facilities.

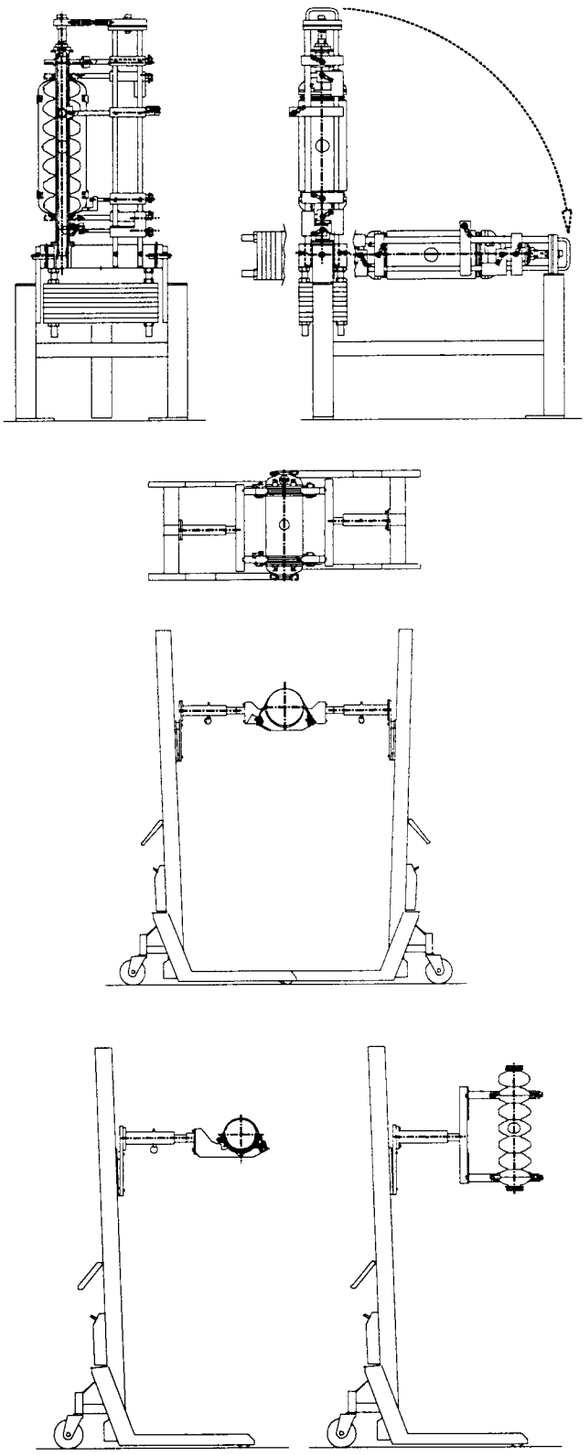

Figure 23: Examples of tooling used in the assembly of the cavity string

5.3 Procedures Development

The fabrication of the Upgrade Cryomodule cavities follows the basic procedures established for the original 4 GeV CEBAF cavities with several modifications:

- Because of the higher performance levels required for the upgraded cavities a more thorough inspection of the starting material is necessary to avoid limitations by inherent material defects. This can be accomplished by making use of the eddy current scanning scheme developed at DESY. [19]
- Because of the absence of bellows in the beamline, close tolerances on the cavity length are needed (+/- 1 mm). This requirement and the desire to manufacture the cavities close to their actual resonance frequency makes it necessary to measure and adjust the half-cell cavity frequencies during the manufacturing process after initial machining.
- The upgraded cavities will have an integrated Ti helium vessel, which will be welded to niobium tuner rings attached to the last cells at each cavity end. Because of pressure vessel code considerations, the baseline design of the helium vessel consists of an approximately 10 in diameter cylinder with Ti bellows and dished heads at each end. The choice of the diameter of the tuner ring does not allow a complete manufacturing of the seven-cell cavity with couplers prior to attaching the He-vessel, but requires first the assembly of the He-vessel and afterwards the attachment of the couplers.

It has been established in several laboratories that more than 100 μm of material must be removed from the inner cavity surface to achieve good cavity performance.[20] In addition, a UHV treatment at ≈ 800 °C removes hydrogen, which can be responsible for "*Q*-disease," from the bulk of the material.[21] The baseline procedures for the upgraded cavity therefore call for the removal of approximately 60 μm of niobium prior to an 800 °C UHV heat treatment; subsequently additional buffered chemical polishing will remove more material.

The final treatment before the vertical qualification test of the seven-cell assembly will be carried out in the new internal chemistry facility located in the Class 100 production clean room, followed by high pressure ultrapure water rinsing, also in a new system located in the same clean room. After a successful vertical test, the cavity assembly will be completed by welding on the Ti He-vessel and the HOM and fundamental power couplers. Final tuning and adjustment of the physical length of the cavity (trimming of beampipes) will be done before the welding.

Prior to assembly of eight cavities to a cavity string, a final chemical treatment has to be given to the cavity surfaces in order to remove any contamination caused by the welding of the He vessel and the couplers. This is again done in the internal chemistry facility. High-pressure rinsing and rinsing with ozonized water is carried out prior to storage of the treated cavity in either water or clean room air. When all eight cavities needed for a string assembly have received their final surface treatments, they will be assembled as quickly and as cleanly as possible assemble into a cavity string, and then pre-aligned and evacuated.

Figure 24 shows the flow of the planned fabrication, treatment, and assembly procedure.

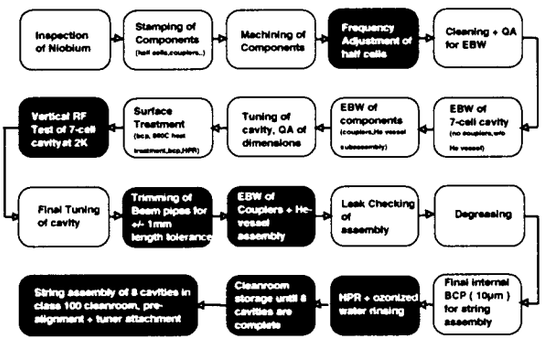

Figure 24: Flow diagram of fabrication, treatment and assembly procedures for Upgrade Cryomodule cavity string (red indicates new procedures, HPR=high pressure rinsing, BCP=buffered chemical polishing).

A program, based on systematic tests on single-cell cavities, is being implemented to assist in the procedures development. [22]

5.4 Electronic Travelers and Database

Work has started on the development of a database aimed at collecting key cavity and cryomodule assembly process information. This database will be constructed using a commercial relational database management system and aimed at easy access to daily critical process information. Data collected can then be analyzed for process trend prediction and generation of performance statistics, and can thereby help formally document progress in the development of the new designs and procedures.

The collection of process information in real time is one aim of this database. The process production tooling and system will be designed and in some cases modified to allow for process information to be gathered electronically on line and placed into the database

directly. In the case of some operations, the data will be manually entered during the processing and assembly stages as the work progresses. In order to allow for easy data entry, the production clean room was wired for Ethernet connection that is routed to the local network. When the system is completed, all key process locations will be wired for connection to the network. At these work locations the users will interface to local personal computer terminals that will allow data to be entered directly into the database.

The data entered by automated processes and users will be stored as tables, designed for each process step. These tables are linked to each other within the database structure to allow users to query any of the various process variables. The results of the query can then be downloaded into graphing and statistical packages to analyze the process or procedures as well as finding the current status a particular component or process.

6 ACKNOWLEDGEMENTS

This paper summarizes the work of the Upgrade Cryomodule Development Team which also includes: I. Campisi, L. Doolittle (now at LBL), E. Feldl, A. Guerra, T. Hiatt, J. Hogan, P. Kneisel, D. Machie, J. Mammosser, G. Myneni, V. Nguyen, L. Phillips, J. Preble, C. Reece, W. Sachleben, W. Schneider, D. X. Wang, M. Wiseman.

7 REFERENCES

1. H. Grunder, "CEBAF Commissioning and Future Plans," PAC95 Proceedings, p. 1.
2. C. Reece et al., "Performance Experience with the CEBAF SRF Cavities," PAC95 Proceedings, p. 1512.
3. C. Reece, "Achieving 800 kW CW Beam Power and Continuing Energy Improvements at CEBAF," Linac98 Proceedings.
4. J. R. Delayen, L. R. Doolittle, and C. E. Reece, "Analysis of Performance Limitations for Superconducting Cavities," Linac98 Proceedings.
5. J. R. Delayen, "Upgrade of the CEBAF Acceleration System," PAC99 Proceedings.
6. L. R. Doolittle, "Strategies for Waveguide Coupling for SRF Cavities," LINAC98 Proceedings.
7. J. R. Delayen, L. R. Doolitle, T. Hiatt, J. Hogan, J. Mammosser, L. Phillips, J. Preble, W. J. Schneider, G. Wu, "An RF Input Coupler System for the CEBAF Upgrade," PAC99 Proceedings.
8. J. R. Delayen, L. Doolittle, E. Feldl, V. Nguyen, W. Sachleben, "Frequency Tuning of the CEBAF Upgrade Cavities," PAC99 Proceedings.
9. J. J. Bisognano, D. R. Douglas, and B. C. Yunn "Alignment Tolerances for CEBAF Accelerating Cavities," CEBAF-TN-91-081, 15 October 1991.
10. D. R. Douglas and J. Preble, "Alignment Tolerance for Seven-Cell SRF Cavity," JLAB-TN-98-022, 22 May 1998.
11. J. R. Delayen, "Phase and Amplitude Stabilization of Beam-loaded Superconducting Resonators,"Linac92 Proceedings.
12. E. Campisi, J. R. Delayen, L. R. Doolittle, P. Kneisel, J. Mammosser, L. Phillips, "Superconducting Cavity Development for the CEBAF Upgrade," PAC99 Proceedings.
13. L. R. Doolittle, D. X. Wang, "RF Control Studies for Moderate Beamline Coupling between SRF Cavities," Linac98 Proceedings.
14. R. C. York, C. Reece, "RF Steering in the CEBAF CW Superconducting Linac", PAC87 Proceedings
15. J. Sekutowicz, 6th Workshop on RF Superconductivity, p. 426, October 1993, CEBAF, Newport News, Va.
16. J. R. Delayen, L. R. Doolittle, E. Feldl, J. Hogan, J. Mammosser, V. Nguyen, L. Phillips, J. Preble, W. J. Schneider, D. X. Wang, M. Wiseman, "Cryomodule Development for the CEBAF Upgrade," PAC99 Proceedings.
17. L. R. Doolittle, "Waveguide Surface Currents," Jefferson Lab tech note.
18. L. Phillips, G. Wu, "Material Properties and Thermal Transitions in RF Couplers," Jefferson Lab tech note.
19. B. Bonin, R. W. Roeth, "Q-degradation of Niobium Cavities due to Hydrogen Contamination," Proc. of the 5th Workshop on RF Superconductivity, DESY Report M 92-01 (April 1992), pp. 210 – 244.
20. W. Singer, D. Proch, A. Brinkmann, "Diagnostic of Defects in High Purity Niobium", Proc. of the 8th Workshop on RF Superconductivity, Abano Terme, Oct. 6–10 1997 Report LNL-INFN(Rep) 133/98 , pp. 850 – 863.
21. E. Mahner, P. Kneisel, N. Pupeter, G. Mueller, "Effect of Chemical Polishing on the Electron Field Emission of Niobium Samples and Cavities," Proc. of the 6th Workshop on RF Superconductivity, CEBAF Oct. 4-8, 1993, pp. 1085 – 1094.
22. P. Kneisel, J. Mammosser, J. R. Delayen; these Proceedings.